

The anti-tumor activity of *Mikania micrantha* aqueous extract in vitro and in vivo

Xiaoju Dou · Yu Zhang · Ning Sun · Yuhe Wu · Li Li

Received: 29 July 2012 / Accepted: 20 November 2012 / Published online: 10 February 2013
© Springer Science+Business Media Dordrecht 2013

Abstract Aqueous extract obtained from *Mikania micrantha* (MMAE) is commonly used as traditional medicine in some countries. We hypothesized that MMAE may inhibit tumor cell growth, both in an in vitro and in vivo setting. In in vitro experiments, two kinds of human cancer cell lines, K562 and HeLa were used to test the anti-tumor activity. Inhibitory concentrations (IC_{50}) were obtained from the inhibition curves fitted by regression analysis, inhibitory rates (%) were calculated by MTT assay, morphological changes were observed by transmission electron microscope (TEM), cell cycles were analyzed by flow

cytometry (FCM), and DNA ladders were determined by agarose gel electrophoresis. The in vivo anti-tumor activity was evaluated by calculating the tumor inhibitory rates, thymus index and spleen index of S180-bearing mice. Paraffin-embedded sections were used to test the pathologic changes. The result displayed that the growth of K562 and HeLa were enhanced when treated with MMAE at 20 $\mu\text{g}/\text{mL}$ after 48 h. Other concentrations of MMAE (50, 100, 200, 400 $\mu\text{g}/\text{mL}$) inhibited the proliferation of both kinds of cells. The IC_{50} values of K562 and HeLa at 48 h were 167.16 and 196.27 $\mu\text{g}/\text{mL}$ and at 72 h 98.07 and 131.56 $\mu\text{g}/\text{mL}$, respectively. The effects showed time-dose dependence. MMAE led to damages of organelles and induced apoptosis. These results were confirmed by ladder DNA fragmentation profile. MMAE also increased the percentage of cells in G2/M phase and decreased the percentage of cells undergoing G0/G1 and S phase in in vivo tests using S180 cells. MMAE showed antitumor activity in vivo, with its tumor inhibitory rate ranging from 12.1 to 46.9 %. MMAE also induced necrosis, as shown by pathological examination of Hematoxylin-Eosin stained tumor sections. Meanwhile, compared with the control group, the changes of thymus index and spleen index in MMAE treated group were not obvious. This study suggests that MMAE may be an effective agent for cancer therapy with low toxicity.

X. Dou
Faculty of Agriculture and Forestry, Tibet Vocational
Technical Collage, Lhasa 850030, China
e-mail: szudou@qq.com

Y. Zhang · L. Li (✉)
College of Life Sciences, Shenzhen Key Laboratory
of Microbial Genetic Engineering, Shenzhen University,
Shenzhen 518060, China
e-mail: ylili@szu.edu.cn

N. Sun
Shenzhen Pass Environmental Testing and Technology
Co.Ltd, Shenzhen 518030, China

Y. Wu (✉)
College of Life Sciences, Shenzhen Key Laboratory
of Marine Bio-Resources and Ecology, Shenzhen
University, Shenzhen 518060, China
e-mail: doudou0918@sohu.com; wuyh@szu.edu.cn

Keywords MMAE (*Mikania micrantha* aqueous extract) · K562 · HeLa · S180-bearing mice

Introduction

Mikania micrantha is one of the 100 worst invasive alien species in the world (Lowe et al. 2001). It was commonly called “mile-a-minute” weed because of rigorous growth habit. This plant originated from South and Central America, has dispersed to South China in the early 1960’s and caused serious damage to crops and forests (Wang et al. 2009).

Rapidly incursive *M. micrantha* competes for water and nutrients, smothers other plants to restrain their photosynthesis, releases phytotoxic compounds which inhibit the growth of neighboring plants and finally kills them (Leung et al. 2009; Simmerloff 2005). Its rampant growth characteristics and allelopathic effects can devastate many native species and cause substantial damage to the ecosystem and biodiversity (Lee et al. 2012).

By GC–MS, water-soluble constituents in MMAE were analyzed and 24 components were identified. The main chemical constituents of *M. micrantha* are sesquiterpene (deoxymikanolide I and dihydromikanolide), flavone (mikanin III, eupalitin IV and stigmaterol- β -D-glucoside V), steroidal (3,4',5,7-tetrahydroxy-6-methoxyflavone 3-O- β -D-glucopyranoside VI) and organic acid (chlorogenic acid) (Wu et al. 2007).

Former research also found out that both aqueous extract and methanol extract of *M. micrantha* could stimulate the expression of CD⁴⁺ and CD⁸⁺, increase the ratio of CD⁴⁺/CD⁸⁺ in mouse. The aqueous extract made notable effects to T lymphocyte compared with methanolic extract. This result indicated that *M. micrantha* could enhance the immune protection and improve the anti-tumor activity (Wu et al. 2005).

Meanwhile, in South American and Southeast Asia, *M. micrantha* is commonly used as traditional medicinal plants and has attracted the attention of natural products chemists because of its antibacterial, antitumor, antimicrobial, cytotoxic and phytotoxic activities (Ghosh et al. 2008; Zhang et al. 2009; Yan et al. 2011).

At present, the invasive character of *M. micrantha* is confirmed, however, most researches are focused on the control, prevention and allelopathy (Weber et al. 2008; Huang et al. 2011). The immunological activity, eco-physiological aspects and genetic structure has also been studied. Nevertheless, the understanding about how to turn the harm of *M. micrantha* into a benefit is still very limited.

In this study, aqueous extract obtained from *M. micrantha* was used to test the anti-tumor activity.

The objectives of this study were to evaluate potential anti-tumor effects of *M. micrantha* by testing (1) growth inhibitory rate of K562 and HeLa, (2) cell cycle changes of K562 and HeLa, (3) changes of cell structure of K562 and HeLa, (4) the tumor inhibitory effect on S180-bearing mice, and (5) pathologic changes of S180-bearing mice.

To the best of our knowledge, this is the first report on anti-tumor activity of *M. micrantha* with the objective to study its pharmacological mechanism. In this research, we demonstrated the anti-tumor activity of *M. micrantha* aqueous extract in vitro and in vivo, providing a promising way for cancer therapy.

Materials and methods

Cells and reagents

The human leukemia cell line (K562) and the human cervical cancer cell line (HeLa), were obtained from Zhongshan Medicine University Cancer Research Resource Center (Guangdong, China). Cells were cultured in RPMI-1640 and DMEM medium, respectively, medium supplemented with 5 % fetal calf serum, 1 % antibiotics (10,000 units/mL penicillin G sodium and 10,000 μ g/mL streptomycin sulfate) and incubated in a 5 % CO₂ incubator at 37 °C.

Cyclophosphamide (CTX), thiazolyl blue (MTT), dimethyl sulfoxide (DMSO), propidium iodide (PI), ethidium bromide (EB) and toluidine blue (TB) were purchased from Sigma–Aldrich (St Louis, MO, USA). RPMI-1640 medium, DMEM medium, fetal bovine serum and antibiotics were from Gibco BRL (Grand Island, NY, USA). Magnesium-free phosphate-buffered saline (PBS) was from Wako Pure Chemical Industries, Ltd. (Osaka, Japan).

Plant materials

Mikania micrantha leaves used in this study were collected from the Plant Garden of Shenzhen University (Guangdong, China), during the rainy season (June to July, 2010 and 2011). The leaves were rinsed with distilled water, dried in a thermostatic oven at 37 \pm 1 °C for 24 h.

Mikania micrantha extract preparation

Aqueous extract of *M. micrantha* (MMAE) was obtained from air-dried plants. 50 g leaves were

weighed out and soaked separately into 200 mL cold water in a conical flask stoppered with rubber corks and left undisturbed for 24 h, then filtered off using sterile filter paper into a clean conical flask and subjected to water bath evaporation, where the aqueous solvent was evaporated at 100 °C (Bhattacharjee et al. 2006). The extract (1,000 mg/mL) was sterilized by 0.22 µm pore membranes and stored as a stock solution at 4 °C for further use (Akuesh et al. 2002).

MTT assay

Concentrations of 5×10^4 K562 cells/mL and 1.5×10^4 HeLa cells/mL were plated in 96-well microtitre plates, respectively, 90 µL in each well. Used medium was replaced with fresh one after 48 h and different concentrations of MMAE were added to the test groups, 10 µL in each well. The final MMAE concentrations were 20, 50, 100, 200, 400 µg/mL. 10 µL of PBS, which contain the same number of cancer cells as the treatment groups, served as control. Wells containing only medium served as blank controls for nonspecific dye reduction. Each concentration was tested in triplicate.

Afterward, plates were incubated at 37 °C in a humidified atmosphere with 5 % CO₂ for 48 and 72 h, respectively. Cells were continuously exposed to MMAE during this period. After incubation, 10 µL of MTT solution (5 mg/mL) was added to each well, plates were incubated in dark for another 4 h, and then centrifuged at 1,000 rpm, 8 min, supernatants were removed by a micropipette and 150 µL DMSO was added in order to dissolve the formazan crystals. The microtiter plates were thoroughly mixed for 5 min, the optical density of each well was measured spectrophotometrically at 570 nm (Biotech Instruments, USA).

The survival rate of tumor cells to each different drug concentrations was calculated as following:

$$\text{Inhibition rate (\%)} = 1 - \frac{\text{OD of drug treated} - \text{OD of blank}}{\text{OD of control} - \text{OD of blank}} \times 100\%$$

The cytotoxicity effects of MMAE on K562 and HeLa cells were determined by measuring the cytotoxic dose that inhibited growth by 50 % (IC₅₀) relative to the control group at 48 and 72 h. The IC₅₀ was obtained from the cytotoxic dose–response curve fitted by probit regression analysis, corresponding to the concentrations of MMAE.

TEM sample preparation

After 48 h of incubation, cells were harvested and immersed in 2.5 % glutaraldehyde in 0.1 PBS (pH 7.4) for 2 h, then postfixed in 2 % osmium tetroxide for another 2 h. The specimens were dehydrated with a graded series of alcohol and propylene oxide, embedded in Epon and stained with TB, examined under TEM (Hitach 600 Electron Microscopy, Japan).

Detection of cell cycle by flow cytometry

After 48 h of incubation, Cells were collected by centrifugation at 1500 rpm for 5 min, then washed twice with PBS. Cells were staining with PI (20 µL of 1 mg/mL stock) in dark at 4 °C for 30 min. The percentages of cellular apoptosis, cells in G0/G1, S, and G2/M phases were analyzed by FCM (Becton–Dickinson, Franklin Lakes, NJ, USA).

DNA fragmentation assay

DNA fragmentation was analysed by agarose gel electrophoresis. Cells were collected using 0.25 % (v/v) trypsin and centrifuged at 2,000 rpm, for 10 min. After washing with PBS, cell pellets were lysed in 800 µL lysis buffer (50 mM Tris–HCl, pH 8, 10 mM EDTA, and 0.3 % Triton X-100) and incubated for 30 min at 0 °C. Cell lysates were treated with RNase (0.1 mg/mL) for 30 min at 37 °C, then treated with proteinase K (0.4 mg/mL) for 1 h at 56 °C. The DNA was precipitated and electrophoresed on 1.5 % agarose gels, visualized with EB (0.5 µg/mL) under UV light.

Animals and treatment

The S180 sarcoma cell line was obtained from the Zhongshan Medicine University Cancer Research Resource Center (Guangdong, China). Four-week-old Balb/c mice were provided by the Zhongshan Medicine University Laboratory Animal Center (Guangdong, China). In total 75 mice, of both sex, weighing 20–22 g at the beginning of the experiments were used throughout the study. Mice were housed separately in polycarbonate cage under a controlled environment of room temperature (20–24 °C) and 40–60 % humidity (relative humidity).

After acclimatization for one week, all mice were inoculated with 0.2 mL S180 sarcoma cells

(1×10^6 cells/mL) into the axilla of the left foreleg, randomly divided into 5 groups, with 15 mice in each one, including the negative control group (gavage with PBS 20 mL/kg b.w.), the low dose group (gavage with MMAE 100 mg/kg b.w.), the moderate dose group (gavage with MMAE 200 mg/kg b.w.), the high dose group (gavage with MMAE 400 mg/kg b.w.) and the positive control group (CTX 50 mg/kg b.w. intraperitoneal injection). All experiments were performed in the same animal facility, no mortality was observed throughout the experiments.

All mice were treated with PBS or MMAE or CTX once a day, for 14 consecutive days. After 14 days of experiment, mice were fasted for 24 h then sacrificed; tumor tissue, thymus gland and spleen were excised and weighed in order to calculate the tumor inhibitory rate, thymus index and spleen index.

The inhibitory rate of S180 tumors, thymus index and spleen index were calculated as follows:

$$\text{Inhibition rate (\%)} = 1 - \frac{\text{Tumor weight in test group}}{\text{Tumor weight in control group}} \times 100 \%$$

$$\text{Thymus index} = \frac{\text{Thymus weight}}{\text{Body weight}} \times 100 \%$$

$$\text{Spleen index} = \frac{\text{Spleen weight}}{\text{Body weight}} \times 100 \%$$

Pathological section preparation

Tumor tissues collected from S180-bearing mice were washed with PBS, fixed with 10 % formalin for 48 h at room temperature. Tissues were trimmed into appropriate size and shape, placed in embedding cassettes for paraffin embedding. The blocks were cut at 5 μm sections, placed in water bath at 40–45 $^{\circ}\text{C}$, the sections were mounted onto slides, dried for 30 min and baked in an oven (45–50 $^{\circ}\text{C}$) overnight.

The deparaffinize sections were fixed in formaldehyde and imbedded by paraffin and stained by Hematoxylin-Eosin (HE). Finally, the sections were observed under a microscope.

Statistical analysis

The results are based on more than three independent experiments. All data are expressed as mean \pm SD. Statistical analysis was conducted using SPSS15.0.

One-way ANOVA, followed by Duncan test, was used to assess the statistical significance of the differences among treatments; $p < 0.05$ was regarded as statistically significant difference; $p < 0.01$ was regarded as highly significant difference.

Results

Effects of MMAE on cell growth

The cytotoxic effect of MMAE was expressed by IC_{50} values. For K562 cells, IC_{50} values were 167.16 and 98.07 $\mu\text{g/mL}$ at 48 and 72 h, respectively. For Hela cells, IC_{50} values were 196.27 and 131.56 $\mu\text{g/mL}$ at 48 and 72 h, respectively (Table 1).

There was an increase in the percentage of cytotoxicity with increasing concentrations of MMAE. MTT assay revealed that different concentrations of MMAE induced time-dose-dependent inhibition (Fig. 1), except for the 20 $\mu\text{g/mL}$ treatment.

We examined the effect of different concentrations (20, 50, 100, 200 and 400 $\mu\text{g/mL}$) on K562 cell growth. The result is reported in Fig. 1a. It revealed that the inhibitory rates were increased when K562 cells were treated with different concentrations of MMAE after 48 and 72 h. Treatment with 200 and 400 $\mu\text{g/mL}$ MMAE made a notable inhibitory effect after 48 and 72 h compared with the control group.

But at a concentration of 20 $\mu\text{g/mL}$ no inhibitory effect occurred. The underlying mechanisms need further research.

The effects of MMAE on Hela cell proliferation is demonstrated in Fig. 1b. Treatment with the concentrations of 200 and 400 $\mu\text{g/mL}$ MMAE made a notable inhibitory effect after 48 and 72 h compared with the control group.

However, the inhibitory effect of MMAE on Hela cells was not as high as for K562 cells. This result indicated that K562 cells exhibited higher sensitivity to MMAE.

Table 1 Growth inhibitory effects of MMAE on K562 and Hela cells at 2 different time points

Cell lines	IC_{50} ($\mu\text{g/mL}$) 48–72 h
K562	167.16–98.07
Hela	196.27–131.56

Changes of cell morphology

As evident in Fig. 2, the treated K562 and Hela cells displayed morphological changes and apoptotic features at various stages compared with untreated cells.

In control group, cells exhibited a normal appearance with large and round morphology; cytoplasm was

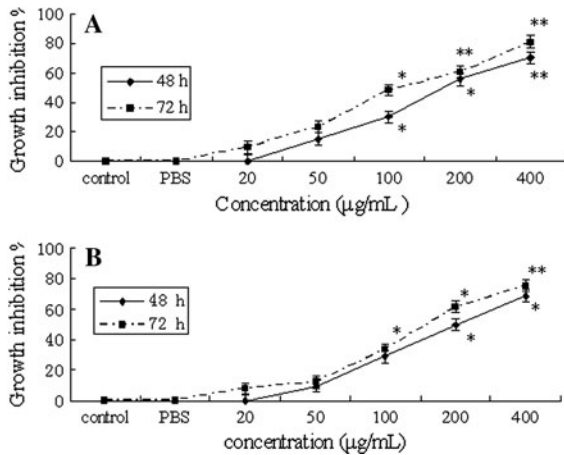


Fig. 1 Growth inhibitory effects of MMAE on K562 and Hela cells **a** K562; **b** Hela, * $p < 0.05$; ** $p < 0.01$

clear with paucity in organelles. Nuclei appeared round to oval, chromatin was finely dispersed (Fig. 2a, c).

However, in the treated group, cell contours were irregular and not well-delimited, the plasma membrane being disrupted and fragmented. The nuclei were irregularly indented, with great variation in shape and size. Mitochondria were swollen, and the mitochondrial membrane was vague or partly ruptured. Chromatin was very dense and conglomerated (Fig. 2b, d).

The morphological changes of K562 and Hela cells were similar. The results obtained from the TEM further confirmed that MMAE induced apoptosis in K562 and Hela cells as demonstrated by the occurrence of apoptotic features.

Effects of MMAE on cell cycle

The effects of MMAE on cell cycle phases were measured in order to obtain information about the cell cycle progression.

The effects of MMAE on cell cycle of K562 are shown in Fig. 3a–f. With the increase of treatment dose, the percentage of cells in G₀/G₁ and S phase decreased and increased in G₂/M phase accordingly,

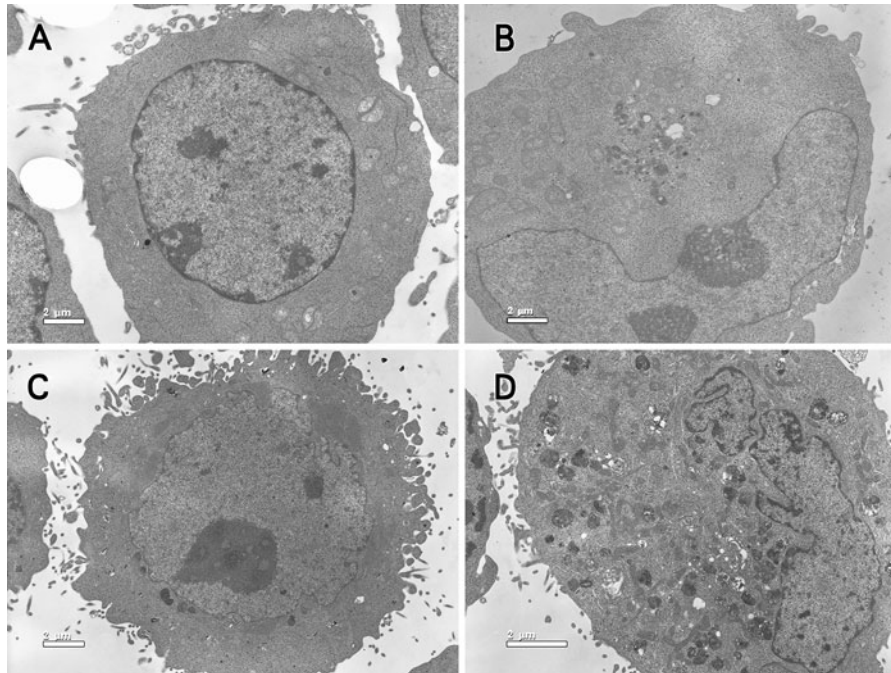


Fig. 2 TEM overview. **a** control group of K562 cells, $\times 3900$; **b** K562 cells treated with 100 µg/mL MMAE, $\times 3900$; **c** control group of Hela cells, $\times 3900$; **d** Hela cells treated with 100 µg/mL MMAE, $\times 3900$

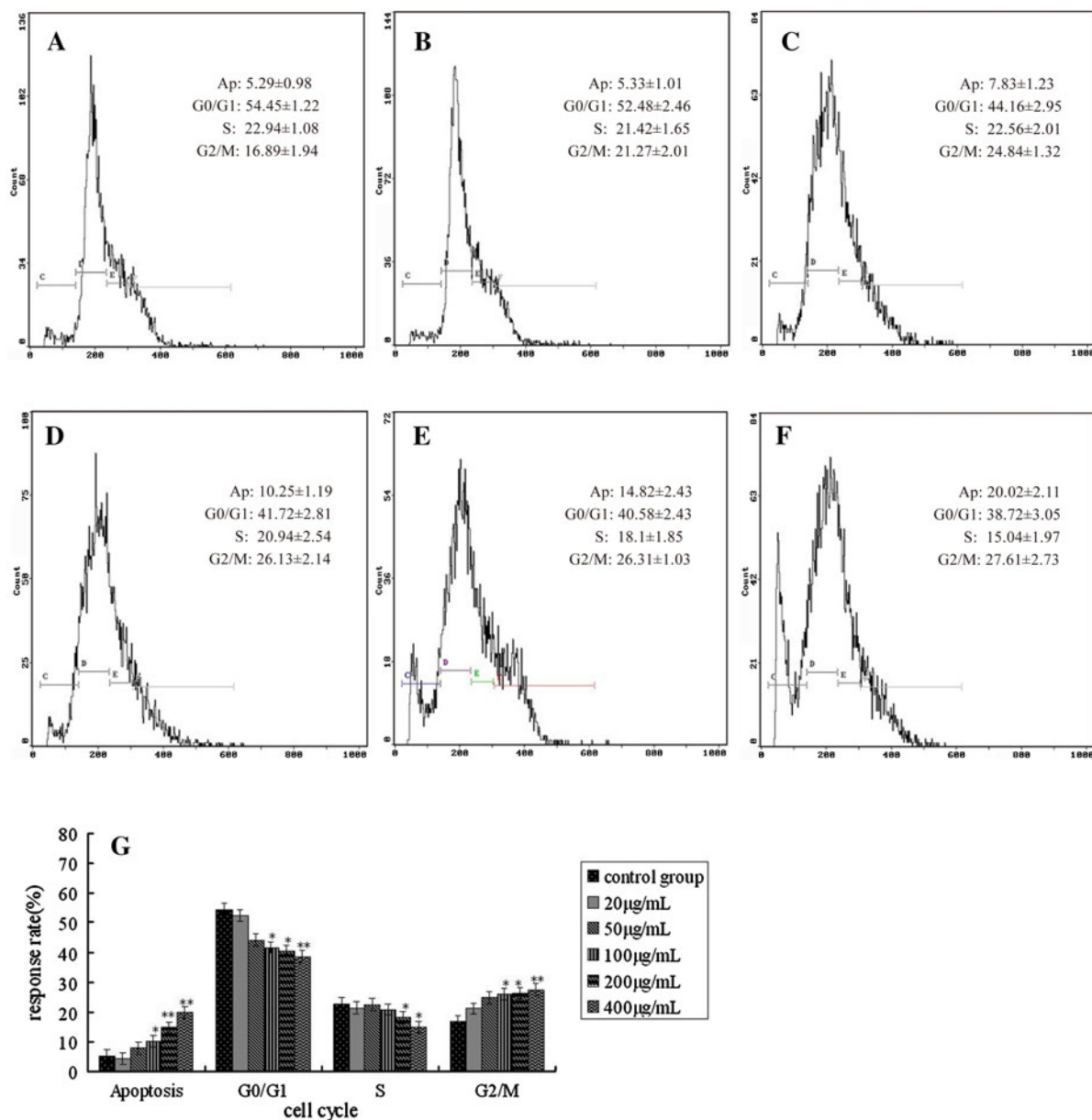


Fig. 3 Effects of MMAE on K562 cell cycle. **a** Control group; **b** 20 µg/mL MMAE; **c** 50 µg/mL MMAE; **d** 100 µg/mL MMAE; **e** 200 µg/mL MMAE; **f** 400 µg/mL MMAE; **g** cell cycle distributions analyzed by Excel, * $p < 0.05$; ** $p < 0.01$

cells showed a block in G2/M phase. The percentage of apoptotic events increased to 20.02 % after the 400 µg/mL treatment (Fig. 3g).

For HeLa cells, a dose dependent effect of MMAE on the cell cycle was observed, as illustrated in Fig. 4a–f. Following 20–400 µg/mL MMAE treatment, there was an increase in the proportion of cells in the G2/M phase and a corresponding decline in the

proportion of cells in G0/G1 and S phase. The results were similar to K562.

DNA ladders of K562 and HeLa

In order to confirm the morphological indications of apoptosis, the DNA bands were analyzed by agarose gel electrophoresis.

At exposure with different concentrations of MMAE (Figs. 5, 6), clear DNA ladders of K562 and Hela cells were observed. The DNA ladders were time dependent and clearly detectable after 48 and 72 h. In contrast, no DNA ladders were visible when treated with 20 µg/mL of MMAE for 48 h. DNA smears were observed in K562 cells treated with 200 µg/mL MMAE after 48 h and in Hela cells treated with 200 µg/mL MMAE after 48 h and 72 h, possibly due to partial degradation of DNA.

Effect of MMAE on S180-bearing mice

As showed in Table 2, inhibition was observed in MMAE treatment at doses of 20–400 mg/kg. The average tumor weights of 3 MMAE groups ranged from 1.31 ± 0.31 g to 0.79 ± 0.22 g. In control group, the tumor weight was 1.49 ± 0.37 g in average. Tumors weight were found to be significantly reduced in the 200 mg/kg group (*p* < 0.05) and highly significantly reduced in the 400 mg/kg group (*p* < 0.01).

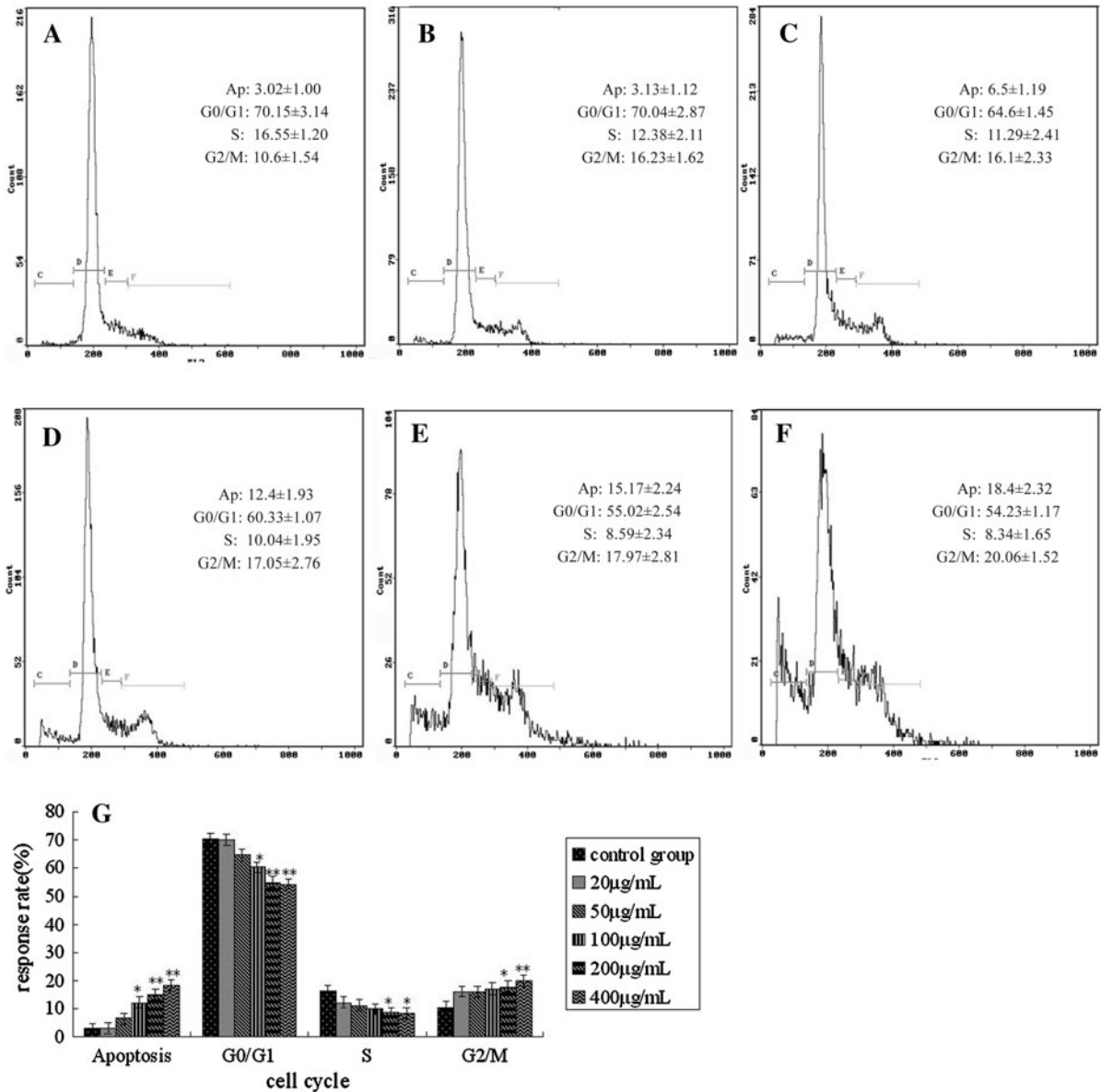


Fig. 4 Effects of MMAE on Hela cell cycle. **a** Control group; **b** 20 µg/mL MMAE; **c** 50 µg/mL MMAE; **d** 100 µg/mL MMAE; **e** 200 µg/mL MMAE; **f** 400 µg/mL MMAE; **g** cell cycle distributions analyzed by Excel, **p* < 0.05; ***p* < 0.01

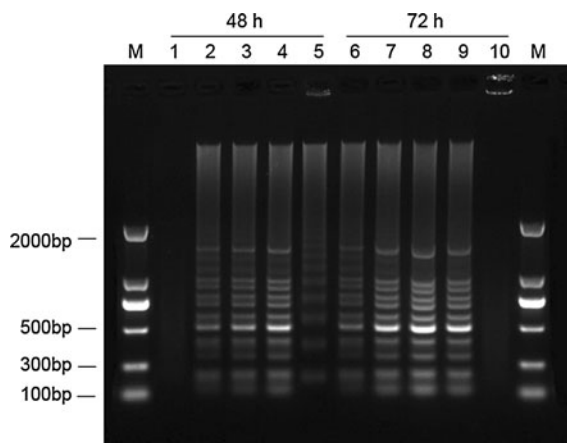


Fig. 5 DNA electrophoretic profiles of K562 cells treated with different concentrations of MMAE after 48 and 72 h. (*M* marker; 1 and 6 20 $\mu\text{g}/\text{mL}$ MMAE; 2 and 7 50 $\mu\text{g}/\text{mL}$ MMAE; 3 and 8 100 $\mu\text{g}/\text{mL}$ MMAE; 4 and 9 200 $\mu\text{g}/\text{mL}$ MMAE; 5 and 10 400 $\mu\text{g}/\text{mL}$ MMAE)

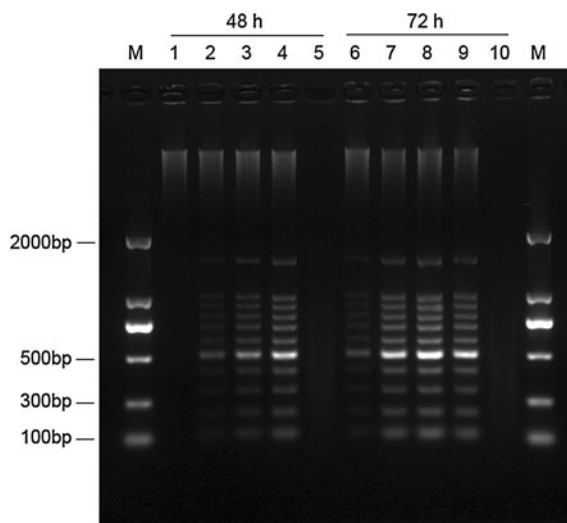


Fig. 6 DNA electrophoretic profiles of HeLa cells treated with different concentrations of MMAE after 48 and 72 h. (*M* marker; 1 and 6 20 $\mu\text{g}/\text{mL}$ MMAE; 2 and 7 50 $\mu\text{g}/\text{mL}$ MMAE; 3 and 8 100 $\mu\text{g}/\text{mL}$ MMAE; 4 and 9 200 $\mu\text{g}/\text{mL}$ MMAE; 5 and 10 400 $\mu\text{g}/\text{mL}$ MMAE)

Moreover, it was obvious that MMAE surpassed CTX in terms of lowered toxicity. The changes of body weights of mice in the MMAE treatment groups were not as significant as for the CTX group. From observations of internal organs, CTX showed a negative influences on spleen index and thymus index ($p < 0.05$), whereas MMAE did not induce such changes.

This result suggested that MMAE did not show obvious toxicity and had little side-effect compared with CTX chemotherapy.

Pathologic changes of S180-bearing mice

Microscopic examination showed that in the control group, tumor cells showed invasive-growth, high level of pathologic mitosis, and no obvious necrosis, nuclei were large, and were heavily stained. The connective tissues were dense, with numerous blood vessels on their surfaces. The boundary region between the tumor and the surrounding normal tissue was very clear (Fig. 7a).

However, after 400 mg/kg MMAE treatment, the results showed large scale cell death with nuclei disappearing, necrotic areas and chipped cells could be found; the structure of tumor cells was collapsed. (Fig. 7b).

Discussion

In this study we tried to reveal the effect of MMAE on the growth of cancer cells and attempted to explore its possible mechanism in vitro and in vivo.

According to former studies, we speculate that the antitumor activity of MMAE may be attributed to the presence of flavonoids, which are known to induce antiproliferative effect.

Flavonoid was expected to be not only a promising cancer-preventive agent contained in foods but also a candidate for chemotherapeutic agents. It has a remarkable spectrum of biological activities that affect the basic cell functions, such as growth, differentiation and apoptosis (Kook et al. 2007). The beneficial effects of flavonoids have been attributed to the inhibition of the enzymes involved in signal transduction as well as to their antioxidant properties (Plazonic et al. 2011).

In the past, satisfactory results have been obtained that flavonoids were able to altering proliferation in cancer cell lines, inducing apoptosis of various tumor cells including K562 (Kuntz et al. 1999). This effect has also been observed in other tumor cell lines from breast, colon and lung carcinomas (Khan and Gilani 2006; Lee et al. 2012). Researches found out that flavonoids inhibited tumor growth through cell cycle arrest and induced apoptosis through a p53-dependent mechanism (Plaumann et al. 1996).

The relationship between concentration of extracts and their inhibitory effects on K562 and HeLa cells

Table 2 Anti-tumor activity of MMAE on S180-bearing mice

Group	Concentration (mg/kg.b.w)	Body weight(g)		Tumor weight (g)	Inhibitory rate (%)	Thymus index	Spleen index
		Beginning	End				
Control group	–	22.94 ± 2.35	28.08 ± 3.04	1.49 ± 0.37	–	3.01 ± 0.34	12.77 ± 1.18
CTX group	20	20.75 ± 1.85*	25.62 ± 2.59*	0.42 ± 0.13**	71.8	1.46 ± 0.96**	9.4 ± 2.27**
Low dose group	100	22.25 ± 1.88	27.46 ± 2.98	1.31 ± 0.31	12.1	3.47 ± 0.64*	11.8 ± 2.86*
Moderate dose group	200	23.32 ± 2.09	28.52 ± 2.66	1.06 ± 0.3*	28.9	3.1 ± 1.52	12.11 ± 3.22
High dose group	400	22.53 ± 1.86	27.71 ± 2.6	0.79 ± 0.22**	46.9	2.97 ± 0.88	12.26 ± 1.71

* $p < 0.05$; ** $p < 0.01$

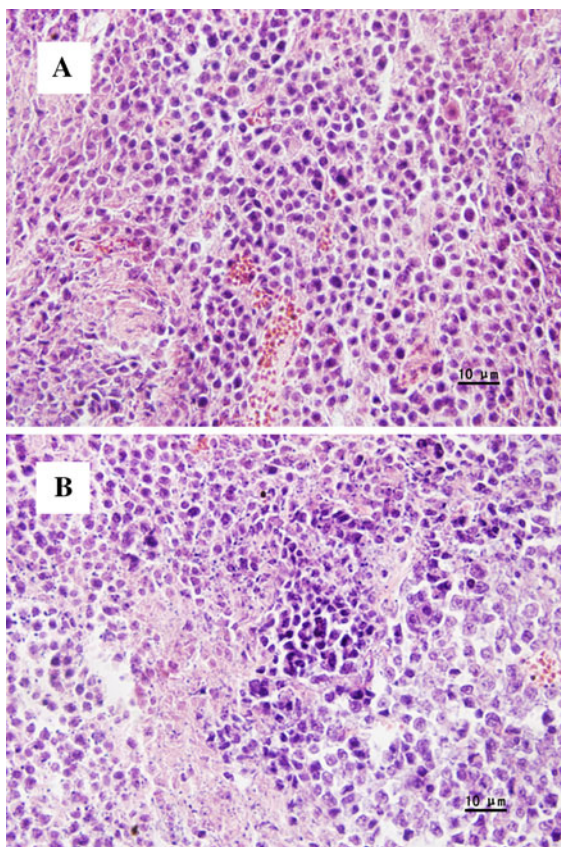


Fig. 7 Pathologic changes of S180 sarcoma tumor. **a** Control group; **b** 400 mg/kg MMAE group

were investigated by MTT assay. MMAE was toxic to K562 and Hela cells at several concentrations in a time-dose-dependent manner. Hela showed a higher tolerance to MMAE than K562. Such different sensitivities perhaps related to the different cellular structure,

perhaps through a protective effect of the microvilli on the cell surface.

Moreover, in our study, at the concentration of 20 $\mu\text{g}/\text{mL}$ MMAE, proliferations of K562 and Hela cells were promoted. Former toxicological studies revealed that there is a dose response phenomenon characterized by low dose stimulation. The possible reasons may be: (1) low concentration regulates gene expression (2) low concentration accelerates metabolism and reproduction of organism (Stebbing 1982). However, the underlying mechanisms need further research.

Apoptosis is the process of programmed cell death that may occur in multicellular organisms. There is a close relationship between apoptosis and cancer occurrence. Apoptosis can be demonstrated by morphological observation, flow cytometry analysis DNA fragmentation.

As detected by TEM, typical morphological changes occurred in the MMAE treatment groups. This demonstrated that MMAE probably exerts its cytotoxic effect by inducing an apoptotic event. Lysosome and mitochondrion are two important organelles which play an essential role in apoptosis.

The lysosome is an organelle that is involved in intracellular digestion, it digests excess or worn-out organelles, participates in cell autolysis and apoptosis process of the lysosomal way (Yang and Cai 2007). As examined under TEM, the number of secondary lysosomes increased significantly in the MMAE treatment groups. The increased lysosomes were able to engulf and remove damaged organelles before the contents spill out to the surrounding cells. This result indicated that MMAE could induce apoptosis by the lysosomal way.

The mitochondrion is another important organelle in cell apoptosis. The mechanisms proposed for mitochondrial involvement in cell death are diverse. In the early stage of apoptosis, single crista in mitochondrion fuses as cristae network, the outer membranes of mitochondrion become permeability. This ionic redistribution leads to an osmotic swelling of the matrix and a consequent rupture of the outer membrane. These changes are considered to be a typical configuration in early apoptosis and usually happen when cells are exposed to certain stimulation (Ma and Zhu 2006).

After MMAE treatment, mitochondrial structures were damaged, crests were fractured and smeared in cytoplasm. This suggests that MMAE could induce apoptosis by damaging mitochondrial structure.

Cell cycle is a key step of cell proliferation. Malignant growth was characterized by uncontrolled cell cycle and loss of cell cycle check points. There are two major check points in cell cycle, the G1/S transition and the G2/M transition (Sun et al. 2011).

Former study revealed that if cells treated with drug could not overcome the G2/M checkpoint, apoptosis would appear (Kim et al. 2007; Theocharis et al. 2004). Our research found out after MMAE treatment, that the number of cells in G2/M phase was increased, while the number of cells undergoing G0/G1 and S phase was decreased. MMAE blocked cell cycle progression at G2/M phase. This indicated that MMAE could inhibit the proliferation of cancer cells by blocking mitosis and damaging the structure of DNA.

Moreover, as expected, the occurrence of apoptosis in treated K562 and Hela cells were further substantiated by DNA ladder. During apoptosis, nuclear chromatin condenses and a calcium dependent endonuclease is activated. DNA fragments into multiples of 180–200 bp. In the MMAE treatment groups, this typical DNA fragmentation pattern occurred and was clearly detectable after 48 and 72 h.

The results obtained from the above experiments confirmed that the MMAE induced apoptosis in K562 and Hela cells as demonstrated by the occurrence of various apoptotic features.

In order to demonstrate the antitumor activity of MMAE *in vivo*, we calculated the tumor inhibitory rates of mice bearing S180. The result showed that both tumor size and weight were decreased after

MMAE treatment. MMAE restrained growth of tumors while it did not interfere with the normal physiological index.

The average volume and weight of transplanted tumors in MMAE treated groups were decreased in comparison to those in the control group, while the tumor necrosis area became larger.

Thymus and spleen are important immunological organs that indirectly reflect humoral immunity. Some kinds of immune inhibitors could cause thymus and spleen atrophy. The relationship between the occurrence, growth of tumor and immune states is an essential problem of tumor immunotherapy (Yuan et al. 2011).

Spleen index and thymus index are the important indications reflecting the immune function of spleen and thymus. The level of its value can reflect the state of immune function.

In clinics, CTX could attack tumor cells, but induces many side effects in the same time. The possible mechanism may relate to damages of immune organs. In the *in vitro* experiment, we got similar results after CTX treatment. But after MMAE treatment, data revealed that all treated groups showed higher immunity index than that of the CTX group. The result indicated that MMAE could retard the deteriorating and atrophic process of immune organs.

Angiogenesis is a process involving endothelial cell sprouting and the formation of new vessels from existing vasculature. Tumors have long been known to depend on angiogenesis to develop, rapidly grow, and successfully metastasize.

As an essential factor of solid tumors progression, the progressive growth and metastasis of malignant neoplasms depend on new blood vessel formation from host vessels. In our study, large scale cell deaths with nuclei disappearing were observed in the MMAE treated groups, in contrast, no such phenomenon was found in the control group.

At the same time, pathological examinations identified spot and minifocal necrosis of tumor cells. Both indicate that MMAE plays a role in solid tumor damages. These data indicate that MMAE is effective in suppressing tumor growth.

Consistent with *in vitro* findings, *in vivo* results also confirmed that MMAE led to a decrease of the growth of tumor tissue with increasing concentrations.

Conclusion

Our data provide evidences that MMAE inhibits the activity of K562 and Hela cells in vitro and the growth of S180 sarcoma cells in vivo through multiple mechanisms including inhibition of proliferation, induction of apoptosis and arrest of cell cycle, while it has low toxicity on immune organs.

As inducing apoptosis has become a new therapeutic target in cancer research, these results suggest that MMAE may have a potential application as a natural antitumor and immunomodulator agent with high efficacy and low toxicity. However, the concentrations selected in the current study are obtained via an in vitro an in vivo study; the possibility to extrapolate these concentrations to clinical practice and anti-tumor mechanisms still needs further investigation.

References

- Akuesh CO, Kadiri CO, Akueshi EU, Agina SE, Ngurukwem B (2002) Antimicrobial potentials of *Hyptis suaveolens* Poit (Lamiaceae). *Niger J Bot* 15:37–41
- Bhattacharjee I, Chatterjee SK, Chatterjee SN, Chandra G (2006) Antibacterial potentiality of *Argemone mexicana* solvent extracts against some pathogenic bacteria. *Mem Inst Oswaldo Cruz* 101:645–648
- Ghosh A, Das BK, Roy A, Mandal B, Chandra G (2008) Antibacterial activity of some medicinal plant extracts. *Nat Med* 62:259–262
- Huang YL, Fang XT, Lu L, Yan YB, Chen SF, Hu L, Zhu CC, Ge XJ, Shi SH (2011) Transcriptome analysis of an invasive weed *Mikania micrantha*. *Biol Plantarum (Suppl)*: e1–e3
- Khan A, Gilani AH (2006) Selective bronchodilatory effect of Rooibos tea (*Aspalathus linearis*) and its flavonoid, chrysoeriol. *Eur J Nutr* 45:463–469
- Kim KY, Ahn JH, Cheon HG (2007) Apoptotic action of peroxisome proliferator-activated receptor- γ activation in human non small-cell lung cancer is mediated via proline oxidase-induced reactive oxygen species formation. *Mol Pharmacol* 72:674–685
- Kook SH, Son YO, Chung SW, Lee SA, Kim JG, Jeon YM, Lee JC (2007) Caspase-independent death of human osteosarcoma cells by flavonoids is driven by p53-mediated mitochondrial stress and nuclear translocation of AIF and endonuclease G. *Apoptosis* 12:1289–1298
- Kuntz S, Wenzel U, Daniel H (1999) Comparative analysis of effects of flavonoids on proliferation, antiproliferativeity and apoptosis in human colon cancer cell lines. *Eur J Nutr* 38:133–142
- Lee SM, Lee YJ, Kim YC, Kim JS, Kang DG, Lee HS (2012) Vascular protective role of Vitexicarpin isolated from *Vitex rotundifolia* in human umbilical vein endothelial cells. *Inflammation* 35:584–593
- Leung GPC, Hau BCH, Corlett RT (2009) Exotic plant invasion in the highly degraded upland landscape of Hong Kong, China. *Biodivers Conserv* 18:191–202
- Lowe S, Browne M, Boudjelas S (2001) 100 of the world's worst invasive alien species, a selection from the global invasive species database. IUCN/SSC Invasive Species Specialist Group (ISSG) Auckland
- Ma T, Zhu QX (2006) Dynamics of Mitochondrial morphology in apoptosis. *Chin J Cell Biol* 28:671–675
- Plaumann B, Fritsche M, Rimpler H, Brandner G, Hess RD (1996) Flavonoids activate wild-type p53. *Oncogene* 13:1605–1614
- Plazonic A, Males C, Mornar A, Nigovic B, Kujundzic N (2011) Characterization and quantification of flavonoid aglucones and phenolic acids in the hydrolyzed methanolic extract of *Caucalis platycarpos* methanolic extract of using HPLC-DAD-MS/MS. *Chem Nat Comp* 47:27–32
- Shao H, Peng SL, Wei XY, Zhang DQ, Zhang C (2008) Potential allelochemicals from an invasive weed *Mikania micrantha* H.B.K. *J Chem Ecol* 31:1657–1668
- Simmerloff D (2005) The politics of assessing risk for biological invasions: the USA as a case study. *Trends Ecol Evol* 20:216–222
- Stebbing ARD (1982) Hormesis—the stimulation of growth by low levels of inhibition. *Sci Total Environ* 22:213–234
- Sun L, Wang Q, Liu X, Brons NHC, Wang N, Steinmetz A, Lv Y, Liao Y, Zheng H (2011) Anti-cancer effects of 20(S)-protopanaxadiol on human acute lymphoblastic leukemia cell lines Reh and RS4; 11. *Med Oncol* 28:813–821
- Theocharis S, Margeli A, Vielh P, Kouraklis G (2004) Peroxisome proliferator-activated receptor- γ ligands as cell-cycle modulators. *Cancer Treat Rev* 30:545–554
- Wang RL, Peng SL, Zeng RS, Ding LW, Xu ZF (2009) Cloning, expression and wounding induction of β -caryophyllene synthase gene from *Mikania micrantha* H. B. K. and allelopathic potential of β -caryophyllene. *Allelopath J* 24:35–44
- Weber E, Sun SG, Li B (2008) Invasive alien plants in China: diversity and ecological insights. *Biol Invasions* 10:1411–1429
- Wu YH, Zhang RL, Hu ZL (2005) Study on the immunological activity of the secondary metabolite in *Mikania micrantha*. *Nat Prod Res Dev* 17:1–4
- Wu YH, Zhu GY, Hong GB, Fang HX (2007) Study on the chemical constituents of *Mikania micrantha*. *J Shenzhen Univ* 24:102–105
- Yan YB, Huang YL, Fang XT, Lu L, Zhou RC, Ge XJ, Shi SH (2011) Development and characterization of EST-SSRs in an invasive weed *Mikania micrantha*. *Am J Bot* 98 (Suppl):e1–e3
- Yang Y, Cai Z (2007) Role of lysosome in cell death. *J Cancer Biother* 14:589–592
- Yuan HM, Song JM, Li XG, Ning L, Liu S (2011) Enhanced immunostimulatory and antitumor activity of different derivatives of κ -carrageenan oligosaccharides from *Kappaphycus striatum*. *J Appl Phycol* 23:59–65
- Zhang LL, Wen DZ, Fu SL (2009) Responses of photosynthetic parameters of *Mikania micrantha* and *Chromolaena odorata* to contrasting irradiance and soil moisture. *Biol Plant* 53:517–522